# ANALYSIS AND OPTIMISATION OF PERIODIC INTERFACE TEXTURES IN THIN-FILM SILICON SOLAR CELLS

B. Lipovšek, M. Cvek, A. Čampa, J. Krč, M. Topič
University of Ljubljana, Faculty of Electrical Engineering,
Tržaška 25, SI-1000 Ljubljana, Slovenia

ABSTRACT: In thin-film silicon solar cells, textured interfaces are introduced to improve light trapping and boost the conversion efficiency. In this work, two-dimensional numerical analysis based on the finite element method is employed to determine the optimal periodic texturisation that can be fabricated on plastic or steel substrate foils. The texturisation is optimised for amorphous silicon (*a*-Si:H), microcrystalline silicon (*μc*-Si:H), and tandem micromorph (*a*-Si:H/*μc*-Si:H) solar cells. Different shapes of periodic features are analysed (rectangular, triangular, sine and U-like), and their lateral and vertical parameters are varied in the optimisation. Simulation results show that optimised periodic textures introduce efficient scattering of long-wavelength light and a pronounced anti-reflective behaviour at shorter wavelengths. While smaller texture features (around 300 nm) are desired for *a*-Si:H cells, larger features (around 1000 nm) are beneficial for *μc*-Si:H and micromorph solar cells. Compared to solar cells deposited on flat substrates, up to 31.6 % (*a*-Si:H cell; absorber thickness 200 nm) and 36.0 % (*i*-*μc*-Si:H cell; absorber thickness 1.2 μm) higher photocurrent can be achieved through optimal substrate texturisation.
Keywords: thin film solar cell, light trapping, simulation, periodic surface-texture

## 1 INTRODUCTION

In thin-film silicon solar cells, efficient light trapping techniques need to be employed in order to boost the absorption in the thin absorber layers and thus increase the conversion efficiency of the cells [1]. For this reason, surface-textured interfaces are introduced into the cell structure to provide light scattering by which the effective optical path lengths through the absorber layers are prolonged. This results in higher generated photocurrent and allows for further reduction of cell thickness. Besides randomly textured interfaces introduced by surface-textured transparent conductive oxide (TCO) substrates or superstrates [2, 3], periodic textures are of interest in the case of flexible plastic or steel substrate foils [4-6]. For the purpose of transferring the periodic textures to the foil substrates, hot embossing (mechanical) [7] and UV embossing (curing UV lacquer) [8] techniques have been developed. The challenge in the design of periodic textures, however, is to determine the optimal shape and dimensions of the texture that would yield the highest gain in solar cell performance.

In this work, numerical simulations based on the finite element method (FEM) are used to analyse and optimise one-dimensional (1-D) periodic textures employed in thin-film amorphous silicon (*a*-Si:H), microcrystalline silicon (*μc*-Si:H), and micromorph tandem (*a*-Si:H/*μc*-Si:H) solar cells. Four types of texture profiles are investigated systematically (Fig. 1): (a) rectangular, (b) triangular, (c) sinusoidal, and (d) U-like. The period of the textures (*P*) and the vertical height (*h*) are chosen as the optimisation parameters. Additionally, in the case of triangular texture, the influence of the duty-cycle (*DC*) which is defined as the ratio of the positive slope to the entire period is also investigated. Based on the simulation results, the optimal periodic textures with respect to the highest improvements in the short-circuit current density ($J_{SC}$) and external quantum efficiency (*QE*) are determined for all three types of thin-film silicon solar cells.

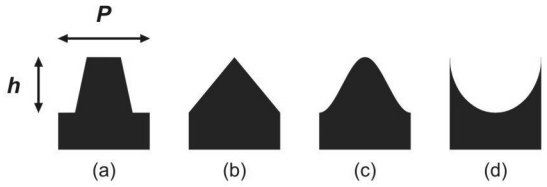


**Figure 1:** The analysed periodic textures: (a) rectangular, (b) triangular, (c) sinusoidal, and (d) U-like. The period (*P*) and height (*h*) parameters are also indicated.

## 2 OPTICAL MODEL

The two-dimensional (2-D) optical simulator FEMOS (Finite Element Method Optical Simulator [9]) was employed to determine the absorption within the individual layers of the solar cell structure. The simulator is based on rigorously solving the Maxwell equations in two dimensions using the finite element method (FEM). Triangular discretisation was used to describe various interface textures, thus avoiding abrupt steps which may occur in the case of rectangular discretisation. As the input parameters, realistic layer thicknesses and complex refractive indices of the materials comprising the cell stack were employed. In order to determine the *QE* and $J_{SC}$ of the solar cell, a simplified but justified electrical analysis was used, assuming ideal extraction of charge-carriers from the intrinsic layer (*i*-*a*-Si:H or *i*-*μc*-Si:H) and neglecting the contributions from *p*- and *n*-doped layers. Under the given assumptions, external *QE* is represented by the simulated wavelength-dependent absorptance in the intrinsic layer, whereas $J_{SC}$ can be calculated from *QE* by applying the AM1.5 spectrum.

## 3 RESULTS AND DISCUSSION

By means of the described optical simulator, the influence of different periodic textures presented in Fig. 1 was studied for *a*-Si:H, *μc*-Si:H and micromorph *a*-Si:H/*μc*-Si:H solar cells. The optimal texture parameters rendering the highest $J_{SC}$ were determined for each cell.

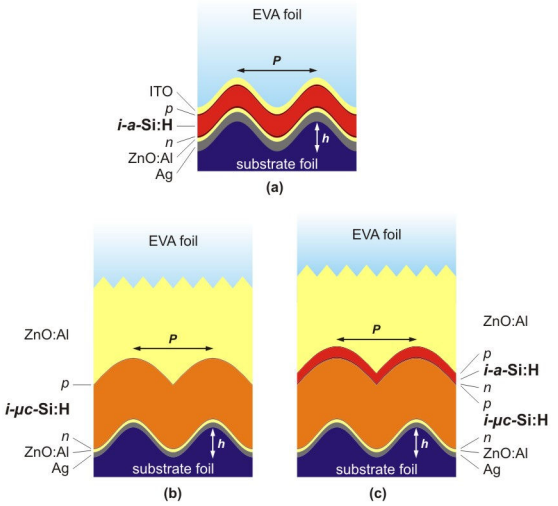


**Figure 2:** The structures of the analysed thin-film silicon solar cells: (a) amorphous *a*-Si:H, (b) microcrystalline *μc*-Si:H, and (c) micromorph tandem *a*-Si:H/*μc*-Si:H cell.

3.1 Amorphous silicon (*a*-Si:H) solar cells

Amorphous silicon solar cells in the following configuration were investigated (Fig. 2a): textured substrate (either plastic or steel foil) / Ag (100 nm) / sputtered ZnO:Al (40 nm) / *n*-*a*-Si:H (20 nm) / *i*-*a*-Si:H (200 nm) / *p*-*a*-SiC:H (15 nm) / ITO (60 nm) / encapsulating EVA foil (incident medium). Due to relatively thin layers of the solar cell, the initial periodic texture of the substrate is considered to be translated to all interfaces of the cell stack. In the simulations, *P* and *h* of the texture were varied in the range of 200 – 1000 nm and 150 – 600 nm, respectively.

In Fig. 3, the optimisation results for the case of sinusoidal periodic texture are presented in terms of relative $J_{SC}$ gains compared to the reference cell with flat interfaces ($J_{SC,\ ref}$ = 11.1 mA/cm$^2$). A well-defined maximum of $J_{SC}$ can be observed at *P* = 300 nm / *h* = 300 nm, indicating a 30.1 % $J_{SC}$ boost compared to the flat cell. Simulations indicate that this combination of *P* and *h* enables efficient light in-coupling at the front interfaces and efficient light scattering in high-angle discrete scattering modes.

The optimal parameters *P* and *h* were determined also for all the other periodic textures. From the results summarised in Table I, similar range of the optimal *P* and *h* values can be observed for almost all the texture profiles. Simulation results show that the triangular periodic texture with *P* = 200 nm, *h* = 300 nm, and *DC* = 0.9 renders the highest $J_{SC}$ increase (31.9 %) compared to the flat cell. Such blazed gratings have been already indicated as promising textures for other types of solar cells [10].

In Fig. 4, the *QE*'s of *a*-Si:H solar cells with the optimal triangular, sinusoidal and rectangular textures (from Table I) are compared together with the *QE* corresponding to the flat cell. From the plot it can be observed that periodic textures significantly improve the performance of the cell in the entire wavelength range. In the short-wavelength region this can mostly be attributed to the pronounced anti-reflective (AR) effect at the front interfaces, whereas in the long-wavelength region *QE* is boosted due to efficient light scattering in combination with the AR effect.

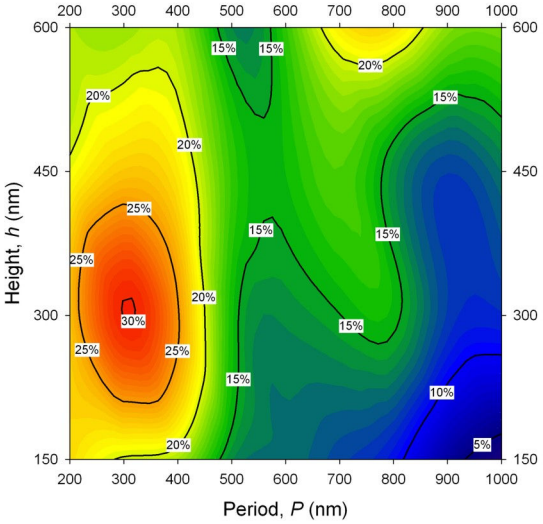


**Figure 3:** Sinusoidal periodic texture: Relative $J_{SC}$ gain compared to the flat *a*-Si:H cell as a function of texture's lateral (*P*) and vertical (*h*) parameters.

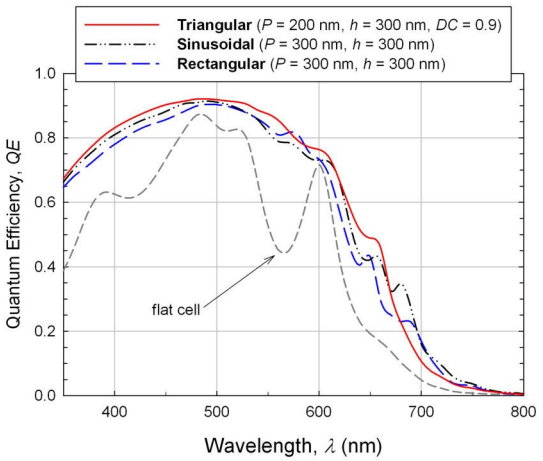


**Figure 4:** Simulated quantum efficiencies of *a*-Si:H solar cells deposited on substrates with different periodic textures. Optimal parameters are chosen for each texture. *QE* results for the flat cell are also shown for reference.

**Table I:** Optimal period and height combinations of periodic surface-textures for *a*-Si:H solar cell with the corresponding $J_{SC}$ gains compared to the flat cell.

| ***a*-Si:H** | | |
|---|---|---|
| Texture | Optimal parameters | Rel. $J_{SC}$ gain |
| Rectangular | *P* = 300 nm<br>*h* = 300 nm | + 25.3 % |
| Triangular<br>(*DC* = 0.5) | *P* = 300 nm<br>*h* = 300 nm | + 27.7 % |
| Triangular<br>(*DC* = 0.9) | *P* = 200 nm<br>*h* = 300 nm | + 31.9 % |
| Sinusoidal | *P* = 300 nm<br>*h* = 300 nm | + 30.1 % |
| U-like | *P* = 800 nm<br>*h* = 600 nm | + 24.6 % |

3.2 Microcrystalline silicon (*μc*-Si:H) solar cells

The configuration of the simulated *μc*-Si:H solar cells was as follows (Fig. 2b): textured substrate / Ag (100 nm) / sputtered ZnO:Al (60 nm) / *n*-*μc*-Si:H (20 nm) / *i*-*μc*-Si:H (1.2 μm) / *p*-*μc*-Si:H (20 nm) / LP-CVD ZnO:Al (2 μm) / encapsulating EVA foil (incident medium). In the case of *μc*-Si:H cells, however, the texture of the substrate foil is changed due to crystalline growth of microcrystalline silicon layers which smoothens the initial roughness [11, 12], as shown in Fig. 2b. This effect of changed morphology on top of the *i*-*μc*-Si:H layer, which is especially pronounced for textures with low-*P*/high-*h* values, was therefore taken into account in our simulations. Additionally, the natural-grown pyramidal roughness of the front LP-CVD ZnO:Al contact was approximated by an appropriately tailored triangular texture, representing the 2-D cross-section of the pyramidal nano-rough surface (also shown in Fig. 2b). To determine the optimal periodic texturisation of the substrate, $J_{SC}$ of the solar cells was simulated for each combination of *P* and *h*, which spanned in the range of 200 – 2000 nm and 300 – 1050 nm, respectively.

In Fig. 5, $J_{SC}$ gains relative to the flat cell ($J_{SC,\ ref}$ = 17.1 mA/cm$^2$) are presented for solar cells deposited on sinusoidal periodic textures with different *P* and *h* parameters. Simulation results indicate the optimal combination of *P* = 1600 nm and *h* = 1050 nm. The values of the texture parameters are much larger than in the case of *a*-Si:H cells. This can be attributed to the fact that in *μc*-Si:H solar cells the important spectral region of light scattering is shifted towards longer wavelengths.

The optimal parameters for all four types of periodic textures are summarised in Table II. The results show that the triangular texture with *P* = 1000 nm, *h* = 900 nm and *DC* = 0.5 is most advantageous, achieving 36.0 % higher $J_{SC}$ than the cell deposited on flat substrate. However, similar results were obtained also for sinusoidal and triangular textures with different *DC* values. The *QE* curves determined for *μc*-Si:H cells with the optimal triangular, sinusoidal and rectangular textures (not shown here) indicate similar trends as those observed for *a*-Si:H cells, most notably the beneficial combination of anti-reflective behaviour in the short-wavelength region and efficient light scattering at longer wavelengths.

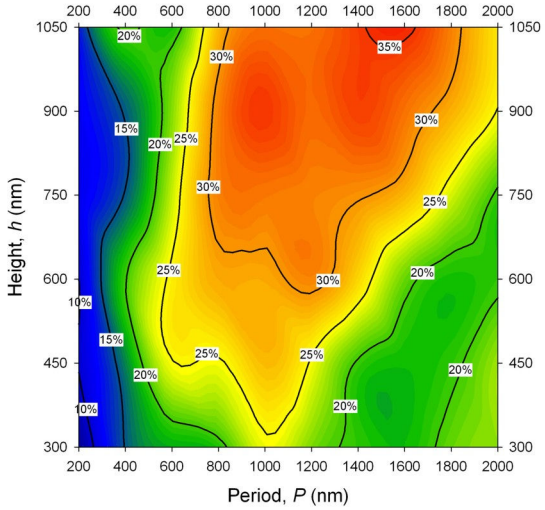


**Figure 5:** Sinusoidal periodic texture: Relative $J_{SC}$ gain compared to the flat *μc*-Si:H cell as a function of texture's lateral (*P*) and vertical (*h*) parameters.

**Table II:** Optimal period and height combinations of periodic surface-textures for *μc*-Si:H solar cell with the corresponding $J_{SC}$ gains compared to the flat cell.

| ***μc*-Si:H** | | |
|---|---|---|
| Texture | Optimal parameters | Rel. $J_{SC}$ gain |
| Rectangular | *P* = 400 nm<br>*h* = 900 nm | + 21.8 % |
| Triangular<br>(*DC* = 0.5) | *P* = 1000 nm<br>*h* = 900 nm | + 36.0 % |
| Triangular<br>(*DC* = 0.9) | *P* = 1200 nm<br>*h* = 900 nm | + 35.9 % |
| Sinusoidal | *P* = 1600 nm<br>*h* = 1050 nm | + 35.7 % |
| U-like | *P* = 1800 nm<br>*h* = 750 nm | + 31.1 % |

3.3 Micromorph tandem (*a*-Si:H/*μc*-Si:H) solar cells

In a micromorph tandem solar cell, the top *a*-Si:H cell absorbs shorter wavelengths (up to ~ 600 nm), while the bottom *μc*-Si:H cell is absorbing at longer wavelengths (up to ~ 1100 nm). In our simulations, the analysed tandem structure was as follows (Fig. 2c): textured substrate / Ag (100 nm) / sputtered ZnO:Al (60 nm) / *n*-*μc*-Si:H (20 nm) / *i*-*μc*-Si:H (1.2 μm) / *p*-*μc*-Si:H (20 nm) / *n*-*a*-Si:H (20 nm) / *i*-*a*-Si:H (200 nm) / *p*-*a*-SiC:H (15 nm) / LP-CVD ZnO:Al (2 μm) / encapsulating EVA foil (incident medium). As before, the initial periodic texture of the substrate foil was changed after the *μc*-Si:H and front ZnO:Al layer deposition. To determine the effects of different periodic substrate textures on $J_{SC}$ of the top and bottom cell, the same *P* and *h* range as in the case of *μc*-Si:H solar cells was investigated.

The simulated *QE*'s for the top and bottom cell are presented in Fig. 6 for triangular, sinusoidal and rectangular periodic textures with *P* = 1000 nm and *h* = 900 nm. The *QE* plot for the flat cell is also shown for comparison. The results indicate that sinusoidal and especially triangular textures significantly enhance the performance of micromorph solar cells, which can mostly be attributed to the anti-reflective effect (top cell) combined with enhanced light scattering capabilities (bottom cell). Rectangular texture with the same *P* and *h* values, on the other hand, is not that beneficial and leads to poorer cell performance.

As shown previously, the optimal features of periodic textures differ significantly for *a*-Si:H and *μc*-Si:H solar cells. While smaller *P* and *h* values are required for *a*-Si:H, larger features are needed for *μc*-Si:H cells. Therefore, in micromorph tandems, the optimisation of the periodic texture with respect to either one of the cells may result in adverse conditions for the other. As an example, if the sinusoidal texture is optimised for the bottom cell (*P* = 1200 nm, *h* = 1050 nm), $J_{SC}$ of the bottom cell is increased by 73.7 %, while $J_{SC}$ of the top cell drops by 6.3 %, compared to the flat cell. Thus, in micromorph tandem solar cells, the optimal texturisation of the substrate foil needs to be designed to best comply with the requirements of both cells in the tandem, rendering the highest cell efficiency.

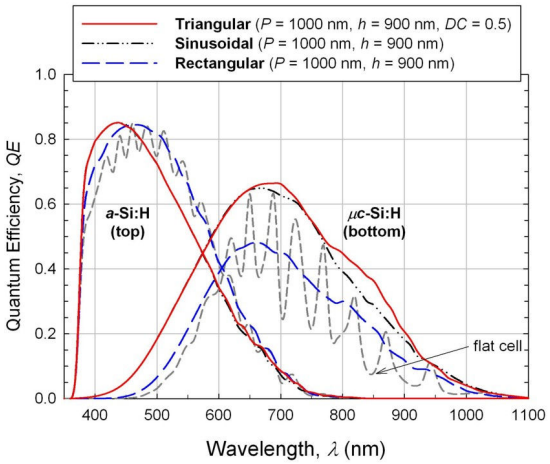


**Figure 6:** Simulated quantum efficiencies of micromorph tandem solar cells deposited on substrates with different periodic textures. *QE* results for the flat cell are also shown for reference.

## 4 CONCLUSIONS

The influence of one-dimensional periodic substrate textures in flexible thin-film amorphous silicon (*a*-Si:H), microcrystalline silicon (*μc*-Si:H), and micromorph tandem (*a*-Si:H/*μc*-Si:H) solar cells was studied by means of optical simulations. The optimal periodic texturisation was determined for each cell. The results indicate that periodic textures reduce total reflectivity and introduce efficient light scattering in *a*-Si:H and *μc*-Si:H solar cells, which leads to $J_{SC}$ increase of up to 31.9 % and 36.0 %, respectively, compared to the flat cells. While smaller lateral and vertical texture features (around 300 nm) are beneficial for *a*-Si:H cells, larger values (around 1000 nm) are desired for *μc*-Si:H and micromorph cells where light scattering at longer wavelengths becomes important.

## ACKNOWLEDGEMENTS

This work was funded by the European FP7 project Silicon-Light (GA No. 241277) and partially by the Slovenian Research Agency (J2-0851-1538-08, P2-0197).

## REFERENCES

[1] A. V. Shah, M. Vanecek, J. Meier, F. Meillaud, J. Guillet, D. Fischer, C. Droz, X. Niquille, S. Fäy, E. Vallat-Sauvain, V. Terrazzoni-Daudrix, J. Bailat, Journal of Non-Crystalline Solids 338 (2004) 639-645.
[2] T. Söderström, F-J. Haug, X. Niquille, C. Ballif, Progress in Photovoltaics 17 (2009) 165-176.
[3] M. Berginski, J. Hüpkes, W. Reetz, B. Rech, M. Wuttig, Thin Solid Films 516 (2008) 5836-5841.
[4] C. Haase, H. Stiebig, Progress in Photovoltaics 14 (2006) 629-641.
[5] F.-J. Haug, T. Söderström, M. Python, V. Terrazzoni-Daudrix, X. Niquille, C. Ballif, Solar Energy Materials & Solar Cells 93 (2009) 884-997.
[6] T. Söderström, F.-J. Haug, V. Terrazzoni-Daudrix, C. Ballif, Journal of Applied Physics 107 (2010) 014507.
[7] M. C. R. Heijna, M. J. A. A. Goris, W. J. Soppe, W. Schipper, R. Wilde, Proc. of 25th EU-PVSEC (2010) 3AV.1.73.
[8] K. Söderström, J. Escarré, O. Cubero, F.-J. Haug, S. Perregaux, C. Ballif, Progress in Photovoltaics: Research and Applications (2010) DOI: 10.1002/pip.1003.
[9] A. Čampa, J. Krč, M. Topič, Journal of Applied Physics 105 (2009) 083107.
[10] R. H. Morf, J. Opt. Soc. Am. A Vol. 12 (1995) 1043-1056.
[11] E. Vallat-Sauvain, J. Bailat, J. Meier, X. Niquille, U. Kroll, A. Shah, This Solid Films 485 (2005) 77-81.
[12] J. Dubail, E. Vallat-Sauvain, J. Meier, S. Dubail, A. Shah, Mat. Res. Soc. Symp. Proc. Vol. 609 (2000).